Analysis of Circumferential Shielding as a Method to Decouple Radio-Frequency Coils for High-Field MRI

Jean-Guy Belliveau[1,2], Kyle Gilbert[1], Mohamed Abou-Khousa[1], and Ravi Menon[1,2]

[1]*Robarts Research Institute, London, Ontario, Canada,* [2]*Biomedical Engineering, University of Western Ontario, London, Ontario, Canada*

Background: When the object being imaged approaches that of the wavelength of the RF coil, multiple element transmit or transmit-receive (transceive) RF coils have been shown to be beneficial for alleviating non-uniformities in the transmit field (using B_1^+ shimming). However, when designing and constructing transmit or transceive arrays, mutual coupling between coil elements (primarily inductive via magnetic field flux linkage) becomes a major concern. This coupling can hinder the ability to B_1^+ shim properly. To decrease coupling between RF coils, decoupling methods such as geometrical overlap and/or capacitive networks can be used; however, their design makes decoupling arbitrary and/or conformal geometries tedious and difficult. These conformal geometries have previously shown that you can potentially improve SNR with receive-only RF coils. Recently, individual shielding in the form of co-planar shields (1,2) and fence like designs (3,4) have been shown increase isolation between elements. This removes the necessity for overlap or electrical connections making each coil act individually and making arbitrary geometries simpler to create. Additionally, shielding to improve efficiency has become prominent at higher frequencies (5,6). However, an investigation of the effects on common performance metrics for RF shielding has not been performed. The following is an investigation into the performance of individual shields by varying the shield the shielding geometry of RF coils at 7 Tesla.

Methods: The geometry of RF coil elements and their respective circumferential shields, as shown in Fig. 1, were altered to investigate the effects on several coil performance metrics. A square phantom (250 x 250 x 125 mm) was filled with a 50-mM NaCl distilled water solution. The width of the circumferential shield (*w*) and the inset of the RF coil (*h*) within the shield were varied. The widths of the RF shields analyzed were 96-mm to 152-mm and unshielded for baseline comparisons. The heights (*h*) of the RF coil was 25-mm to 51-mm (increased in 3-mm increments). SNR ratio maps between shielded and unshielded RF coils were calculated to view the effects of shielding. SNR ratios were calculated for simulations where a value of 1 indicates a 100% increase in SNR for the shielded coils and a value of -1 indicates a 100% decrease in SNR for shielded coils. Peak local SAR was calculated using the IEEE 1528.1 built in CST macro on power matched RF coils. These values were subsequently corrected by using a voltage normalization term, ensuring a consistent flip angle between all RF coils analyzed. Coupling between two coils was measured by placing two coils of identical geometry side-by-side in the axial plane and measuring S_{21}. SNR measurements with the second coil acting as a perturbing element were also acquired to analyze the effect of coupling on SNR.

Results: SNR ratio maps for the imaging experiments are shown in Fig. 2 (a-d). The focusing of the field patterns increases the SNR within the widths of the shields. However, the narrow shields have a faster drop of SNR gains compared to wider shields. The rapid drop off of the SNR outside of the shields also indicated that adjoining coils should be more orthogonal compared to the unshielded coils increasing B_1^+ shimming and parallel MRI abilities. Peak local SAR is highest for the narrowest shield due to the field focusing; however, a normalization voltage correction (7) must be applied to the simulated data to ensure the flip angle used is consistent for all coils compared. The voltage correction was applied in post-processing to create B_1^+ maps with a normalized flip angle in a power calibrated voxel. The voltage correction value is lowest for narrow shields at a depth of 10-mm indicating a higher efficiency for that particular geometry and lowest for the widest shield at a depth of 60-mm. The voltage correction squared is then used to compute the corrected peak local SAR values (also shown in Table 1) for a consistent flip angle. Coupling between two coils was measured to be between -6.5 dB to -22.1 dB. Coupling is decreased by increasing the inset of the RF coil (*h*) for narrow shielding or by widening the shields. High coupling between RF coils not only decreases the depth penetration of SNR for the RF coils, but reduces the orthogonality of the elements and causes unwanted excitation underneath the perturbing coil (up to 60% of max SNR).

Conclusion: There are trade-offs for designing shielded RF coils. Narrower shields may increase SNR in the periphery of the brain for imaging of the cortex and allow for a denser concentration of RF coils. Wider shields should be used for deep structure imaging as depth penetration of the wider shields is increased. Shielded elements also constrain the field patterns to within the RF shields, allowing for increased orthogonality between elements and potential increase in B_1^+ shimming capabilities or parallel MRI reconstruction. These results can be applied to various shielding schemes.

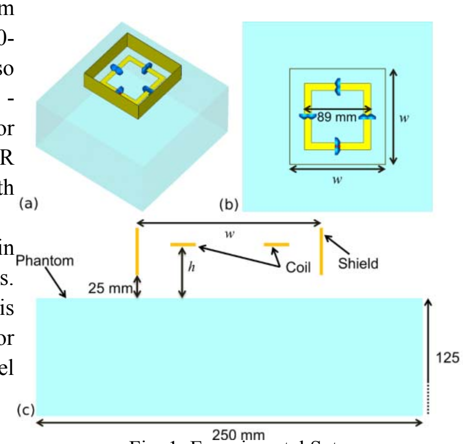

Fig. 1: Experimental Setup

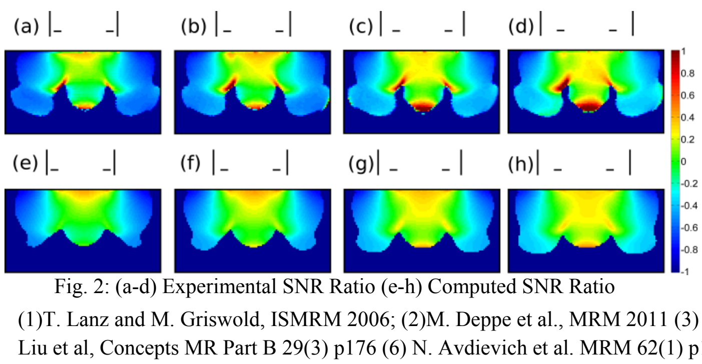

Fig. 2: (a-d) Experimental SNR Ratio (e-h) Computed SNR Ratio

Coil Height (mm)	Peak Local SAR (W/kg)	Voltage / SAR Correction 10 mm deep voxel	Voltage / SAR Correction 60 mm deep voxel
104	3.01	0.114 / 0.0391	0.681 / 1.40
114	2.96	0.118 / 0.0412	0.668 / 1.32
127	2.85	0.124 / 0.0438	0.660 / 1.24
140	2.71	0.130 / 0.0458	0.656 / 1.17
Unshielded	1.79	0.166 / 0.0493	0.793 / 1.12

Table 1: Peak local SAR and corresponding corrected values

(1)T. Lanz and M. Griswold, ISMRM 2006; (2)M. Deppe et al., MRM 2011 (3) C. Leussler, U.S. Patent 1644922010; (4) K. Gilbert et al. MRM 64(6) p1640; (5) W. Liu et al, Concepts MR Part B 29(3) p176 (6) N. Avdievich et al. MRM 62(1) p17 (7) Collins et al. MRM 45(4) p684